DESIGN AND TESTING OF A FULL-DEGREE-OF-FREEDOM CONSTRAINED SEED GUIDING DEVICE FOR ORDERED SEED FLOW

/

有序种子流全自由度约束导种装置设计与试验

Xin DU*, Qianhao YU, Shufa CHEN, Qixin SUN, Yue JIANG, Jingyi MAO
Jiangsu Ocean University, Lianyungang 222005/ China
Tel: 0086-0518-85895322; E-mail: xindu@jou.edu.cn
Corresponding author: Xin Du
DOI: https://doi.org/10.35633/inmateh-76-14

Keywords: *Precision seeding; Seed guiding device; High-speed; Precision agriculture*

ABSTRACT

To improve the uniformity and stability of seed guidance in ordered seed flow and meet the requirements of precision sowing operations, a brush-type seed guiding device capable of constraining all degrees of freedom of the seeds was designed. Bench tests were conducted to optimize the factors affecting performance, namely the nut-bolt head spacing, the brush-to-housing gap, and the brush belt speed. Through single-factor experiments, the influence of each factor on seed guidance performance was clarified, and reasonable value ranges were determined. Combined with a response surface test, a multiple quadratic regression model was established to describe the relationship between these factors and the variation coefficients of pass rate, missed seeding rate, and seed spacing. The results show that optimal seed guidance performance is achieved when the nut-bolt head spacing is 39.15 mm, the brush-to-housing gap is 0.22 mm, and the brush belt linear velocity is 0.644 m/s. This study provides a theoretical foundation and data support for the development of precision sowing technology and its associated seed guiding devices.

摘要

为提高有序种子流导种均匀性与稳定性，满足精量播种作业要求，设计了一种可约束种子全部自由度的毛刷式导种装置，对影响其工作性能的螺母-螺栓头间距、毛刷-外壳间隙和毛刷带线速度等因素进行了台架试验优化。通过单因素实验阐明各因素对导种性能的影响规律，并确定因素的合理取值范围。结合响应面试验，建立了各因素与合格率、漏播率和粒距变异系数间的多元二次回归模型。结果表明，当螺母-螺栓头间距为 39. 15 ㎜、毛刷-外壳间隙为 0. 22 ㎜、毛刷带线速度为 0. 644 m/s 时，导种性能最佳。本研究可为精量播种技术及配套导种装置的研制提供理论基础与数据支撑。

INTRODUCTION

In 2024, the corn planting area and total output in China reached 44.74 million hectares and 294.92 million tons, respectively, consistently securing the top position among the three major grain crops for several years. Nevertheless, China's corn yield remains at only 6.59 tons per hectare, significantly lower than the 11.11–12.04 tons per hectare achieved by the United States and other developed countries (*Awad et al., 2022*). The full mechanization of corn sowing in China has made sowing quality a critical factor influencing corn yield (*Liao et al., 2020*). While significant research has focused on precision seed metering devices within single-seed sowing technology, studies specifically addressing the seed guiding mechanism remain scarce (*Du et al., 2023*). As a result, the seed guiding process has become a limiting factor in improving the quality of high-speed sowing operations. This highlights an urgent need for the development of an efficient seed guiding mechanism tailored to high-speed sowing requirements (*Fanigliulo et al., 2022*).

The seed guiding device is a core component of precision seeders, directly influencing seeding accuracy and efficiency, particularly at high operating speeds. To overcome this bottleneck, recent research has focused on optimizing seed guide designs to improve seed motion stability and placement accuracy.

Xin Du, Lecturer Ph.D. Eng; Qianhao Yu, MA.Eng Stud.; Shufa Chen, Prof. Ph.D. Eng; Qixin Sun, Prof. Ph.D. Eng; Yue Jiang, Lecturer Ph.D. Eng.; Zhanrui Zhang, B.S Stud.*

Key technological strategies include:

Pneumatic-assisted seed guiding: utilizing airflow to guide and constrain seed trajectories. Examples include air-delivery auxiliary seed guides (*Li et al., 2025*), guidance restraint-airflow blowing devices (*Liu et al., 2025*), and conical spiral airflow high-speed guides (*Zhang et al., 2024*). These systems improve seeding uniformity through the optimization of airflow parameters (*Karayel et al., 2022*). Internationally, companies like Amazone and Vaderstad employ positive-pressure airflow ejection mechanisms. Air-assisted guidance has also been adapted for specialized applications, such as hill-seeding of sesame (*Wang et al., 2023*). Mechanical structure optimization: Researchers have developed novel geometries aimed at minimizing seed bouncing and collisions. These include converging groove-guided seed tubes (*Jia et al., 2024*), seed tubes based on the brachistochrone principle (*He et al., 2022*; *Li et al., 2024*), and belt-type systems. For example, *Chen et al. (2012)* designed a belt-based mechanism to ensure precise seed trajectory and improved spacing uniformity, while *Liu et al. (2017)* developed a sowing synchronous belt device for systematic seed transport to the seedbed. Performance monitoring and simulation: Employing technologies like photoelectric sensors for real-time monitoring of belt-type devices (*Wang et al., 2024*) and leveraging DEM-CFD coupling for advanced design and optimization (*Li et al., 2024*; *Ma et al., 2023*).

Despite being the most prevalent mechanism currently, the reliance of the gravity-based seed guide tube (*Im et al., 2023*) on seed descent along the inner wall induces significant bouncing and spacing non-uniformity at high operating speeds. This limitation highlights the urgent need for continued optimization through pneumatic assistance, innovative mechanical designs (including belt-type systems), and simulation-monitored approaches. While scholars domestically and internationally have made progress in mitigating the seed guide's impact on spacing consistency (*Du et al., 2024*; *Kumar-Patel et al., 2021*; *Ospanova et al., 2024*), persistent challenges remain in effectively preventing collisions between seeds and the seeding mechanism's inner wall, particularly under high-speed conditions. These collisions disrupt the initial stable seed flow, leading to uneven spacing, reseeding, or seed loss.

To address this specific bottleneck, this study introduces a seed discharge mechanism engineered for orderliness and smoothness, employing full-degree-of-freedom constraints. The core objective is to minimize spacing deviations induced within the seed guiding process itself, thereby refining precision sowing theory and advancing seeding machinery toward higher speed and precision.

MATERIALS AND METHODS

Overall structure and working principle

This study introduces an advanced mechanism for the high-speed and seamless delivery of maize, employing a fully constrained seed guiding system with a full range of degrees of freedom. This innovative approach is integrated with a high-speed precision seed discharger designed in the preceding phase (*Du et al., 2023*). The comprehensive configuration of both the seed discharger and the delivery mechanism is illustrated in Figure 1. The structure primarily consists of the following components: mounting base, housing, seed cleaning brush, air inlet, seed inlet, internal filling plate, brush belt drive motor, inner filling plate drive motor, compression spring, seed pushing wheel, belt-driver wheel, brush belt housing, brush belt, timing belt, belt-driven wheel, tensioning device, and coupling.

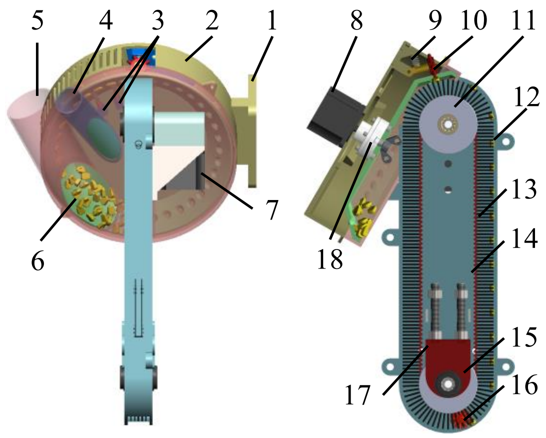

Fig. 1 – Schematic diagram of the structure of the seed-guiding device

1. Mounting base; 2. Housing; 3. Seed cleaning brush; 4. Air inlet; 5. Seed inlet; 6. Inner charging disk; 7. Brush belt drive motor; 8. Inner charging disk drive motor; 9. Pressure spring; 10. Seed pushing wheel; 11. Active belt wheel; 12. Brush belt housing; 13. Brush belt; 14. Synchronous belt; 15. Passive belt wheel; 16. Seed combing rollers; 17. Tensioning device; 18. Coupling

During operation, maize seeds are guided into the seed-filling chamber through the seed inlet by the seed dispenser. The filling process begins with the clockwise rotation of the inner filling disk, driven by a motor via a coupling. Under the combined effects of gravity, centrifugal force, inter-seed interaction, and airflow pressure, seeds are guided into designated holes. Excess seeds are removed by the seed cleaning brush and returned to the filling chamber, ensuring that each hole contains only one seed. Next, the seed tray advances to the seed pushing area, where the air holes at the bottom align with the seed holes to create a sealed path. The seed pushing wheel then rotates, pressing the seeds out of the holes and embedding them into the brush belt. The bristles of the brush constrain the seed's movement, securing it within the guiding system. Driven by a motor, the brush belt transports the seed to the seed outlet. There, the brush housing opens to release the seed, completing the guided delivery process.

Test design

This study utilized "Zhengdan 958" maize seeds as the experimental material to evaluate seed guiding performance, employing the JPS-12 multifunctional seeding test platform. To simulate the relative motion between seeds and the ground during field sowing, the seed guiding device was securely mounted onto the stationary frame of the test platform. The platform's conveyor belt was operated at linear speeds ranging from 3.6 km/h to 14.4 km/h. To minimize seed bounce and displacement upon landing, a 1-2 mm layer of grease was applied to the belt surface. The experimental setup is shown in Figure 2.

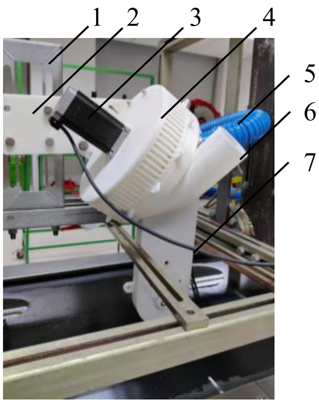

Fig. 2 – Schematic diagram of the bench test of the seed-guiding device

1. seed dispenser fixing frame; 2. seed dispenser fixing plate; 3. seed dispenser drive motor; 4. pneumatic seed dispenser; 5. air inlet pipe; 6. seed inlet; 7. seed guiding device

Test indicators

To assess the operational effectiveness of the seed-guiding device, evaluation criteria based on GB/T 6973-2005 were employed. The evaluation focused on criteria such as qualification, multiplicity, and missed seeding rate. The calculation formulas for each performance index are as follows:

To evaluate the operational performance of the seed-guiding device, assessment criteria were applied in accordance with the national standard GB/T 6973-2005. The evaluation focused on key performance indicators, including qualification rate, multiple seeding rate, and missed seeding rate. The calculation formulas for each performance index are presented below:

$$\begin{cases} Y_1 = \dfrac{n_1}{N} \times 100\% \\ Y_2 = \dfrac{n_0}{N} \times 100\% \\ X_a = \dfrac{\sum_{i=1}^{N-1} X_i}{N-1} \\ C = \dfrac{\sqrt{\dfrac{\sum_{i=1}^{N-1} X_i \left(X_i - X_a\right)^2}{N-1}}}{X_a} \times 100\% \end{cases} \tag{1}$$

Y_1 is the qualified rate, %; Y_2 is the missed seeding rate, %; X_a is the average seed spacing, cm; C is the coefficient of variation of seed spacing, %; n_1 is the number of qualified seed holes (holes); n_0 is the number of empty holes (holes); N is the total number of seed holes tested (251 holes); X_i is the distance between two adjacent seeds, cm.

After conducting three repetitions for each treatment, involving the statistical analysis of 251 holes within corn seed rows, average values were calculated. The data was then organized to derive the qualified rate, missed seeding rate and coefficient of variation of seed spacing (COV).

RESULTS

Influence of synchronous belt tension

The tension of the synchronous belt was adjusted by regulating the distance between two left-handed bolt heads and a nut, as illustrated in Figure 3(a). To evaluate the seeding performance of the synchronous belt under varying tension conditions, a one-factor bench test was conducted at an operating speed of 10 km/h and an air pressure of 1.6 kPa. The experimental variable was the distance between the nut and the bolt head, which was set at five levels: 38.0 mm, 38.5 mm, 39.0 mm, 39.5 mm, and 40.0 mm. The objective was to assess the qualified seeding rate, multiple seeding rate, and missed seeding rate of the seed discharging mechanism. The test results are presented in Figure 3(b).

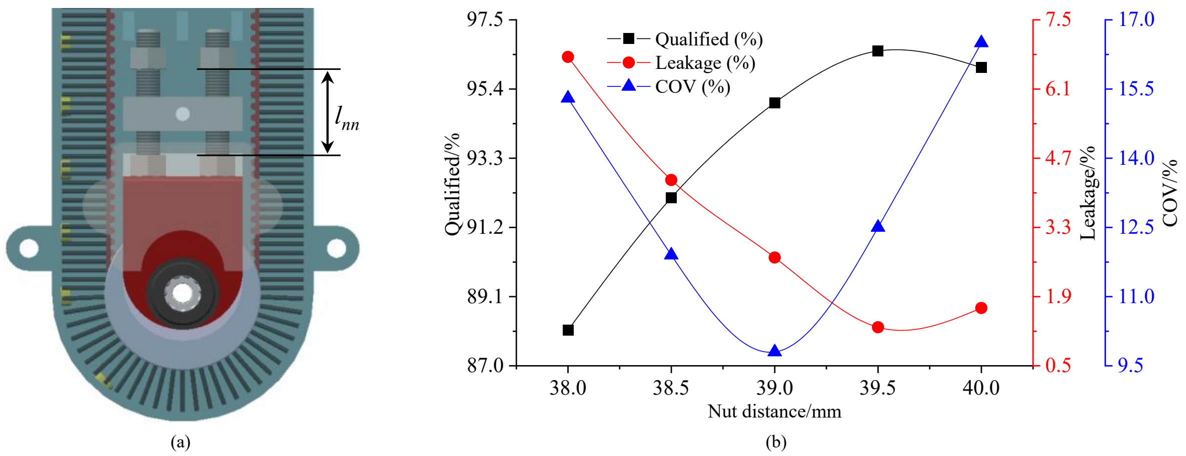

Fig. 3 – Tension adjustment-nut distance and effect of nut spacing on seed displacement performance

As depicted in Figure 3(b), the qualified rate shows a gradual increase with an increment in the distance between the nut and the bolt head. This phenomenon arises because heightened tension prevents the drive belt from easily skipping teeth, facilitating a smoother movement of the bristles carrying the seed. Consequently, this smoother movement reduces the likelihood of seed displacement from the bristles, resulting in decreased missed seeding and reseeding rates. Notably, when the distance between the nut and the bolt head reaches 40.0 mm, the rates of single seed, reseeding, and missed seeding are comparable to those at 39.5 mm, yet the tension force becomes excessively high.

As shown in Figure 3(b), the qualified seeding rate increases progressively with the expansion of the distance between the nut and the bolt head. This trend is attributed to the increased belt tension, which minimizes the risk of tooth-skipping by the drive belt and promotes smoother motion of the bristles that transport the seeds. Improved motion stability reduces the likelihood of seed displacement from the bristles, thereby lowering both missed seeding and multiple seeding rates. However, when the distance reaches 40.0 mm, the qualified, missed, and multiple seeding rates are similar to those observed at 39.5 mm, although the resulting belt tension is excessively high, potentially introducing mechanical strain or inefficiencies.

Influence of brush-housing gap

As shown in Figure 4(a), the clearance between the bristles of the brush belt and the housing plays a critical role in maintaining seed positioning accuracy during transportation. If the gap is too wide, seeds may become dislodged due to vibrations during movement. Conversely, if the gap is too narrow, excessive friction and resistance between the bristles and the inner wall of the housing can hinder the normal operation of the drive belt. To investigate this effect, a one-factor bench test was conducted at an operating speed of 10 km/h and an air pressure of 1.6 kPa. The gap between the bristles and the housing was adjusted to five levels: -2 mm, -1 mm, 0 mm, 1 mm, and 2 mm. The results are presented in Figure 4(b).

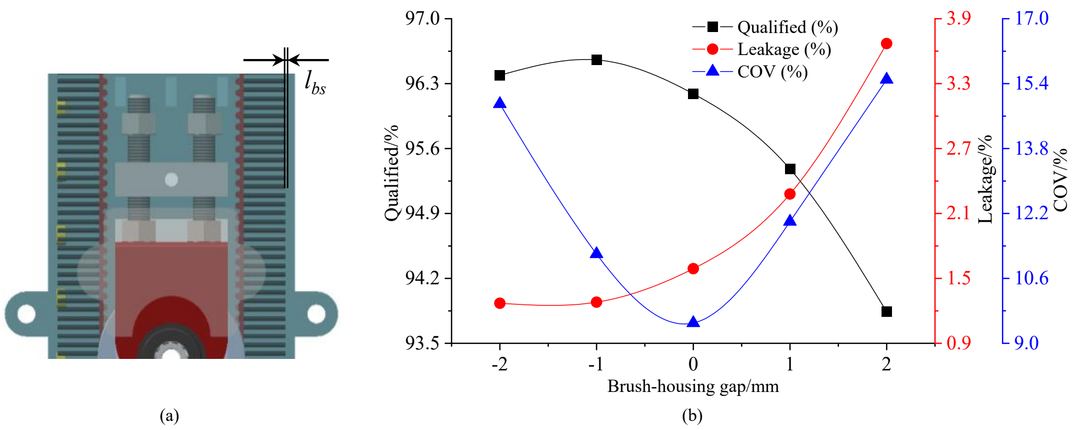

Fig. 4 – Schematic diagram of the clearance between the bristles and the housing, and the effect of the bristle-housing gap on seed discharge performance

As illustrated in Figure 4(b), an excessively large gap results in seed dislodgement during transport, leading to increased missed seeding and multiple seeding rates. Conversely, when the gap is too small, the multiple seeding rate also increases - likely due to the seeds being tightly wrapped by the bristles, which hinders their timely release during the discharge process. Notably, when the gap was set to -1 mm, the qualified seeding rate reached its highest value, while both the multiple and missed seeding rates were at their lowest. Therefore, -1 mm is identified as the optimal bristle-housing gap for ensuring stable and accurate seed discharge performance.

Influence of brush belt linear speed

A single-factor bench test was conducted under the conditions of a 10 km/h operating speed, 1.6 kPa air pressure, and a bristle-to-housing clearance of -1 mm. The test variable was the linear speed of the brush belt, set at five levels: 0.3 m/s, 0.6 m/s, 0.9 m/s, 1.2 m/s, and 1.5 m/s. The results of this test are shown in Figure 5.

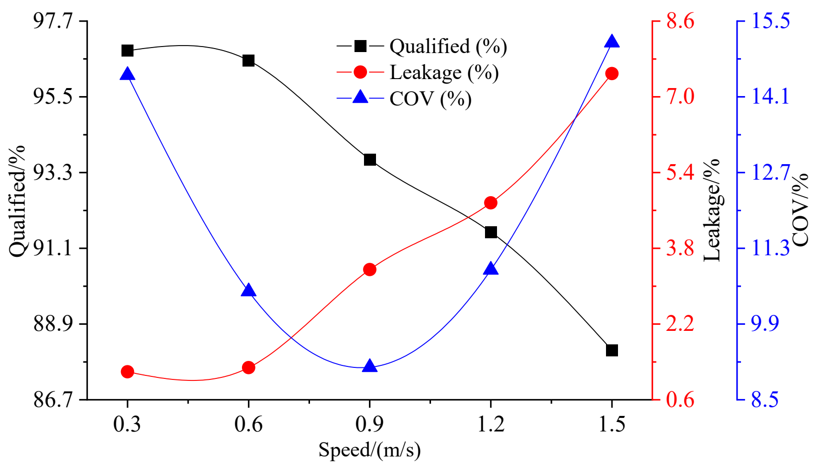

Fig. 5 – Influence of brush belt linear speed on seed displacement performance

As shown in Figure 5, a gradual decline in the qualified seeding rate is observed with increasing brush belt linear speed. This trend is attributed to the increased relative motion between the seed discharge disk and the brush belt, which hampers the ability of the seed pushing wheel to accurately embed seeds into the bristles in a timely manner. As a result, both missed seeding and multiple seeding rates increase. At a brush belt speed of 0.6 m/s, the seed guiding device achieves its highest qualified seeding rate, along with the lowest rates of multiple and missed seedings.

Interactions among the factors

To investigate the interaction effects of nut-bolt head spacing, brush-housing gap, and brush belt linear velocity on seed guiding performance, a Box–Behnken experimental design was employed. The study focused on three performance indicators - qualified seeding rate, missed seeding rate, and seed spacing uniformity - to quantitatively assess the influence of each factor and their interactions on the seed guiding mechanism.

The test scheme and test results are shown in Table 1.

Table 1

Box-Behnken test program and results

No.	l_{nn} (mm)	l_{bs} (mm)	v_m (m/s)	Y_1 (%)	Y_2 (%)	C (%)
1	38	-2	0.9	86.61	6.45	17.6
2	40	-2	0.9	94.01	2.82	17.2
3	38	2	0.9	84.57	5.17	15.6
4	40	2	0.9	92.51	4.78	15.1
5	38	0	0.3	88.36	3.82	14.2
6	40	0	0.3	95.17	2.39	16
7	38	0	1.5	81.61	9.12	19.1
8	40	0	1.5	89.71	6.49	16.4
9	39	-2	0.3	96.58	2.08	15.2
10	39	2	0.3	95.22	2.86	12.5
11	39	-2	1.5	90.66	6.92	17.1
12	39	2	1.5	89.26	7.02	15.8
13	39	0	0.9	94.98	2.69	9.8
14	39	0	0.9	94.74	2.94	9.9
15	39	0	0.9	95.23	2.49	9.6
16	39	0	0.9	94.83	2.43	9.7
17	39	0	0.9	95.13	2.82	9.8

The results of the ANOVA for the qualification rate are shown in Table 2.

Table 2

ANOVA results for qualification rate

Source	Sum of Squares	df	Mean Square	F Value	P value
Model	308.68	9	34.30	864.07	< 0.0001**
A-A	114.38	1	114.38	2881.65	< 0.0001**
B-B	4.96	1	4.96	124.99	< 0.0001**
C-C	72.54	1	72.54	1827.53	< 0.0001**
AB	0.07	1	0.0729	1.84	0.2175
AC	0.42	1	0.4160	10.48	0.0143*
BC	0.0004	1	0.0004	0.01	0.9229
A^2	100.57	1	100.57	2533.60	< 0.0001**
B^2	1.89	1	1.89	47.58	0.0002**
C^2	8.04	1	8.04	202.67	< 0.0001**
Residual	0.28	7	0.0397		
Lack of Fit	0.11	3	0.0376	0.91	0.5110
Pure Error	0.17	4	0.0413		
Cor Total	308.96	16			

*Note: ** indicates highly significant (p<0.01) and * indicates significant (p<0.05).*

A quadratic multiple regression was fitted to the qualified rate to obtain the regression equation:

$$Y_1 = -7465.72 + 384.50 l_{nn} - 3.02 l_{bs} - 19.07 v_m + 0.07 l_{nn} l_{bs} + 0.54 l_{nn} v_m - 0.01 l_{bs} v_m - 4.89 l_{nn}^2 - 0.17 l_{bs}^2 - 3.84 v_m^2 \quad (2)$$

The interaction effects of brush belt speed and nut-bolt head spacing on the qualified seeding rate are illustrated in Figure 6. As the brush belt speed increases, the qualified rate of the seed guide shows a gradual decline. In contrast, with increasing nut-bolt head spacing, the qualified rate initially rises and then falls. Overall, the optimal seed guiding performance is achieved when the brush belt speed is between 0.3 and 0.6 m/s and the nut–bolt head spacing is between 39 mm and 40 mm.

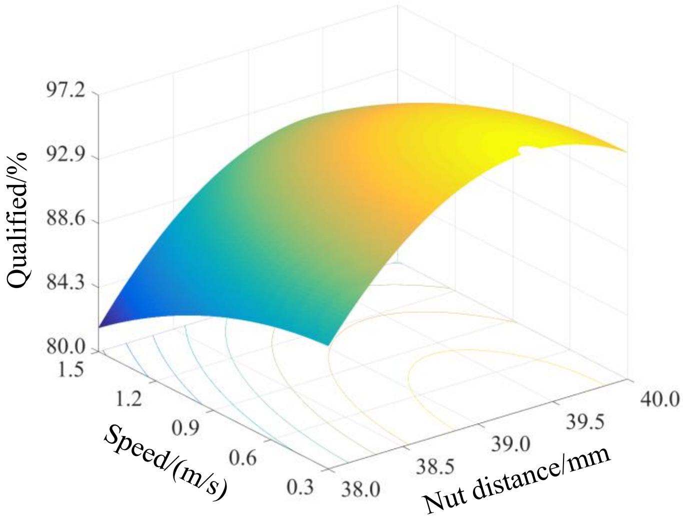

Fig. 6 – Response surface analysis of the interaction effects of factors

The results of the ANOVA for the missed seeding rate are shown in Table 3.

Table 3

ANOVA results for missed seeding rate

Source	Sum of Squares	df	Mean Square	F Value	P value
Model	74.16	9	8.24	273.48	< 0.0001**
A-A	8.16	1	8.16	270.84	< 0.0001**
B-B	0.30	1	0.30	10.10	< 0.0001**
C-C	42.32	1	42.32	1404.51	< 0.0001**
AB	2.62	1	2.62	87.10	< 0.0001**
AC	0.36	1	0.36	11.95	0.01**
BC	0.12	1	0.12	3.84	0.09
A^2	8.65	1	8.65	286.95	< 0.0001**
B^2	2.05	1	2.05	68.08	< 0.0001**
C^2	7.65	1	7.65	253.92	< 0.0001**
Residual	0.21	7	0.03		
Lack of Fit	0.03	3	0.01	0.18	0.9042
Pure Error	0.19	4	0.05		
Cor Total	74.37	16			

*Note: ** indicates highly significant (p<0.01) and * indicates significant (p<0.05).*

A quadratic multiple regression was fitted to the missed seeding rate to obtain the regression equation:

$$Y_2=2203.69-112.33l_{nn}-15.57l_{bs}+16.59v_m+0.41l_{nn}l_{bs}-0.50l_{nn}v_m-0.14l_{bs}v_m+1.43l_{nn}^2+0.17l_{bs}^2+3.74v_m^2 \quad (3)$$

The interaction effects of the brush-housing gap and nut-bolt head spacing on the missed seeding rate are shown in Figure 7(a). As the brush-housing gap increases, the missed seeding rate gradually rises. In contrast, with increasing nut-bolt head spacing, the missed seeding rate first decreases and then increases. Overall, the lowest missed seeding rate is observed when the brush-housing gap is between -2 mm and -1 mm, and the nut-bolt head spacing is within the range of 39-40 mm.

The interaction effects of brush belt speed and nut-bolt head spacing on the missed seeding rate are presented in Figure 7(b). The missed seeding rate increases progressively with higher brush belt speeds. Similarly, as the nut-bolt head spacing increases, the missed seeding rate initially decreases and then increases. In general, optimal performance - with the lowest missed seeding rate - is achieved when the brush belt speed is maintained between 0.3 and 0.6 m/s, and the nut-bolt head spacing is in the range of 39-40 mm.

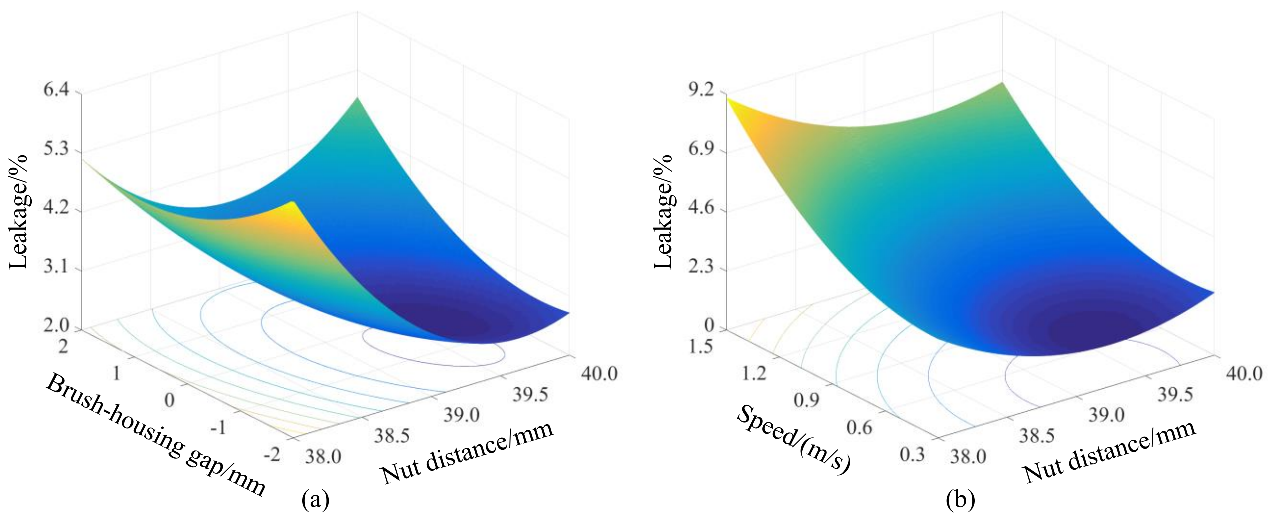

Fig. 7 – Response surface analysis of the interaction effects of factors

The results of the ANOVA for the COV are shown in Table 4.

Table 4

ANOVA results for COV

Source	Sum of Squares	df	Mean Square	F Value	P value
Model	168.81	9	18.76	2409.08	< 0.0001**
A-A	0.41	1	0.41	52.02	0.0002**
B-B	8.20	1	8.20	1053.37	< 0.0001**
C-C	13.78	1	13.78	1770.07	< 0.0001**
AB	0.003	1	0.003	0.32	0.59
AC	5.06	1	5.06	650.23	< 0.0001**
BC	0.49	1	0.49	62.94	< 0.0001**
A^2	65.53	1	65.53	8416.51	< 0.0001**
B^2	30.02	1	30.02	3855.32	< 0.0001**
C^2	31.15	1	31.15	4001.07	< 0.0001**
Residual	0.05	7	0.008		
Lack of Fit	0.003	3	0.0008	0.06	0.9761
Pure Error	0.05	4	0.013		
Cor Total	168.86	16			

*Note: ** indicates highly significant (p<0.01) and * indicates significant (p<0.05).*

A quadratic multiple regression was fitted to the COV to obtain the regression equation:

$$C=5957.22-306.25l_{nn}-0.28l_{bs}+61.71v_{m}-0.01l_{nn}l_{bs}-1.88l_{nn}v_{m}+0.29l_{bs}v_{m}+3.95l_{nn}^{2}+0.67l_{bs}^{2}+7.56v_{m}^{2} \quad (4)$$

The interaction effects of brush belt speed and nut-bolt head spacing on the COV of seed spacing are shown in Figure 8(a). The COV initially decreases and then increases with rising brush belt speed and nut-bolt head spacing. The lowest COV values are observed when the speed is between 0.6 and 0.9 m/s and the nut-bolt head spacing ranges from 38.5 to 39.5 mm. Figure 8(b) illustrates the interaction effects of brush belt speed and brush-housing gap on the COV. A similar trend is observed: the COV decreases at first and then increases with increasing values of both variables. The optimal performance - reflected by the lowest COV - is achieved when the brush belt speed is between 0.6 and 0.9 m/s and the brush-housing gap is between -1 mm and 1 mm.

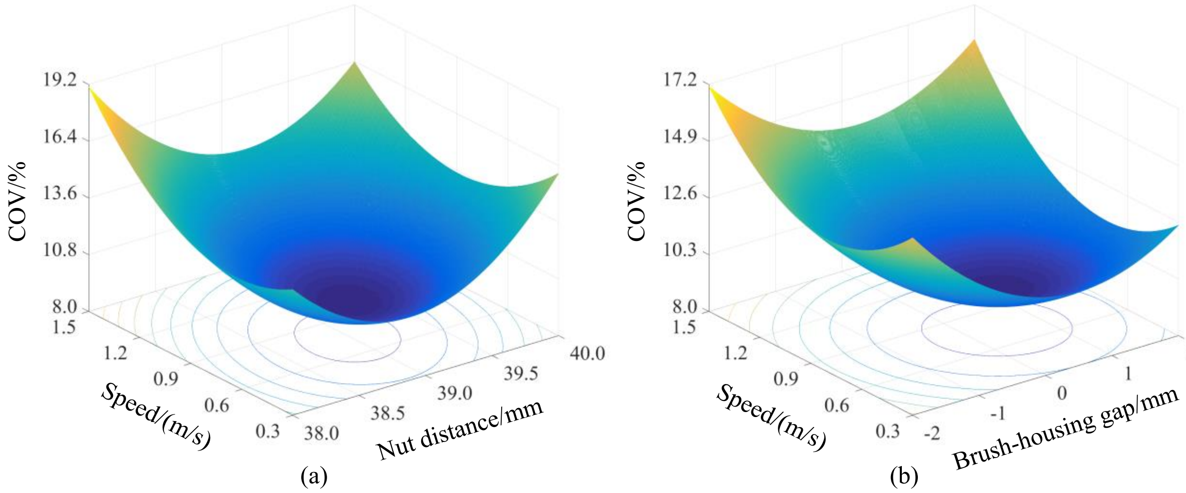

Fig. 8 – Response surface analysis of the interaction effects of factors

To identify the optimal combination of influencing factors within the defined constraint ranges, a multi-objective optimization was performed based on the regression model of seed guiding performance. The evaluation indices included the maximum qualified seeding rate, the minimum missed seeding rate, and the minimum coefficient of variation (COV) of seed spacing.

The optimization problem was formulated with the objective function and corresponding constraints defined as follows:

$$\begin{cases} \max Y_1\left(l_{nn}, l_{bs}, v_m\right) \\ \min Y_2\left(l_{nn}, l_{bs}, v_m\right) \\ \min C\left(l_{nn}, l_{bs}, v_m\right) \\ s.t.\begin{cases} 38 \text{ mm} \le l_{nn} \le 40 \text{ mm} \\ -2 \text{ mm} \le l_{bs} \le 2 \text{ mm} \\ 0.3 \text{ m/s} \le v_m \le 1.5 \text{ m/s} \end{cases} \end{cases} \tag{5}$$

The regression model was optimized and solved using Design-Expert 10 software. The optimal parameter combination was found to be a nut-bolt head spacing of 39.15 mm, a brush-housing gap of 0.22 mm, and a brush belt speed of 0.644 m/s. Under these conditions, the predicted values for the qualified seeding rate, missed seeding rate, and COV were 96.35%, 1.89%, and 9.72%, respectively. To validate the model, the bench test was repeated three times using the optimized parameters. The experimental results yielded a qualified seeding rate of 96.76%, a missed seeding rate of 2.15%, and a COV of 10.09%. The close agreement between the predicted and measured values confirms the high reliability and accuracy of the regression model.

CONCLUSIONS

This study aimed to address the problem of seed bouncing and displacement caused by collisions between corn seeds and the seed guide tube during planting, which disrupts the orderly flow of seeds. To overcome this issue, a seed guiding device was developed to constrain the seeds in all degrees of freedom, utilizing a flexible brush to ensure stable seed transport. A one-factor test was conducted to determine the optimal parameter ranges for nut-bolt head spacing, brush-housing gap, and brush belt speed, and to evaluate their individual effects on seed guiding performance. Subsequently, quadratic regression models were established using response surface test to analyze the effects of these parameters on the qualified seeding rate, missed seeding rate, and COV. Optimization results indicated that the best seed guiding performance was achieved at a nut-bolt head spacing of 39.15 mm, a brush-housing gap of 0.22 mm, and a belt speed of 0.644 m/s, resulting in a qualified seeding rate of 96.35%, a missed seeding rate of 1.89%, and a COV of 9.72%.

ACKNOWLEDGEMENT

This study was supported by Natural Science Foundation of Jiangsu Province (BK20241058), and the Project of Graduate Student Scientific Research and Practical Innovation Program of Jiangsu Ocean University (KYCX2024-41).

REFERENCES

[1] Awad, M., Fouda, O., Abd el-reheem, S., ABD El-reheem, S., Al-gezawe, A., Cottb, M., Okasha, M. (2022). A new seed drill for planting peas on a raised-bed. *INMATEH - Agricultural Engineering,* Vol. 68, pp. 681-692. https://doi.org/10.35633/inmateh-68-67

[2] Chen, X., Zhong, L. (2012). Design and test on belt-type seed delivery of air-suction metering device (气吸式排种器带式导种装置的设计与试验). *Transactions of the Chinese Society of Agricultural Engineering*, Vol. 28, pp. 8-15.

[3] Du, X., Yu, Q., Chen, S., Sun, Q., Zhang, H., Liu, C. (2024). Design and testing of seed push wheel for high-speed precision seed metering device for corn with internal seed filling and positive pressure airflow. *INMATEH - Agricultural Engineering*, Vol. 72, pp. 731-740. https://doi.org/10.35633/inmateh-72-65

[4] Du, X., Liu, C. (2023). Design and testing of the filling-plate of inner-filling positive pressure high-speed seed-metering device for maize. *Biosystems Engineering*, Vol. 228, pp. 1-17.

[5] Fanigiliulo, R., Grilli, R., Benigni, S., Fornaciari, L., Biocca, M., Pochi, D. (2022). Effect of sowing speed and width on spacing uniformity of precision seed drills. *INMATEH - Agricultural Engineering,* Vol. 66, pp. 9-18. https://doi.org/10.35633/inmateh-66-01

[6] He, C., JIN, X., LU, L., Ma, M., Wang, X., Zhang, J. (2022). Design and experiment on seed-guiding tube of T-groove furrowing device based on brachistochrone. *INMATEH - Agricultural Engineering*, Vol. 67, pp. 53-66. https://doi.org/10.35633/inmateh-67-05

[7] Im, D., Lee, H., Kim, J., Moon, D., Moon, T., Yu, S., Park, Y. (2023). Bucket size optimization for metering device in garlic planter using discrete element method. *Agriculture (Basel),* Vol. 6, pp. 1199, Korea.

[8] Jia, X., Zhu, J., Guo, G., Huang, Y., Gao, X., Zhang, C. (2024). Design and test of a novel converging groove-guided seed tube for precision seeding of maize. *Biosystems Engineering*, Vol. 245, pp. 36-55.

[9] Karayel, D., Güngör, O. & Šarauskis, E. (2022). Estimation of optimum vacuum pressure of air-suction seed-metering device of precision seeders using artificial neural network models. *Agronomy (Basel),* Vol. 7, pg. 1600.

[10] Kumar-Patel, S., Bhimani, J. B., Yaduvanshi, B. K., Gupta, P. (2021). Optimization of the design and operational parameters of planter for vegetable pigeon pea (*cajanus cajan l. millsp*.) seed. *INMATEH - Agricultural Engineering,* Vol. 63, pp. 326-334. https://doi.org/10.35633/inmateh-63-33

[11] Li, H., Yang, L., Zhang, D., Cui, T., He, X., Xie, C., Li, C., Du, Z., Xiao, T., Li, Z., Wang, H. (2024). Design and optimization of a high-speed maize seed guiding device based on DEM-CFD coupling method. *Computers and Electronics in Agriculture*, Vol. 227, pp. 109604.

[12] Li, Y., Zhou, W., Ma, C., Feng, Z., Wang, J., Yi, S., Wang, S. (2024). Design and optimization of the seed conveying system for belt-type high-speed corn seed guiding device. *International Journal of Agricultural and Biological Engineering*, Vol. 17, pp. 123-131.

[13] Li, Z., Zhang, H., Huang, J., Lou, C., Chen, Y., Liu, L., Zhang, T., Chen, L. (2025). Design and parameter optimization of air-delivery auxiliary seed guide for pneumatic plate precision rapeseed metering device. *Computers and Electronics in Agriculture*, Vol. 230, pp. 109840.

[14] Liao, Y., Li, C., Liao, Q., Wang, L. (2020). Research progress of seed guiding technology and device of planter (播种机导种技术与装置研究进展分析). *Transactions of the Chinese Society for Agricultural Machinery*, Vol. 51, pp.1-14.

[15] Liu, Q., He, X., Yang, L., Zhang, D., Cui, T., Qu, Z., Yan, B., Wang, M., Zhang, T. (2017). Effect of travel speed on seed spacing uniformity of corn seed meter. *International Journal of Agricultural and Biological Engineering*, Vol. 10, pp. 98-106.

[16] Liu, R., Zhang, G., Xiao, Y., Yan, B., Meng, Z., Dong, J., Wu, G. (2025). DEM-CFD investigation of particle motion characteristic in a guidance restraint-airflow blowing seed guiding device. *Advanced Powder Technology*, Vol. 36, pp. 104747.

[17] Ma, C., Yi, S., Tao, G., Li, Y., Wang, S., Wang, G., Gao, F. (2023). Research on receiving seeds performance of belt-type high-speed corn seed guiding device based on discrete element method. *Agriculture (Basel)*, Vol. 13, pg.1085.

[18] Ospanova, S., Aduov, M., Kapov, S., Orlyansky, A., Volodya, K. (2024). The results of experimental research of a rotor seed-metering unit for sowing non-free-flowing seeds. *Journal of agricultural engineering (Pisa, Italy),* Vol. 55, pg.1556.

[19] Wang, B., Liao, Q., Wang, L., Shu, C., Cao, M., Du, W. (2023). Design and test of air-assisted seed-guiding device of precision hill-seeding centralized seed-metering device for sesame. *Agriculture (Basel)*, Vol. 13, pg. 393.

[20] Wang, S., Yi, S., Zhao, B., Li, Y., Wang, G., Li, S., Sun, W. (2024). Photoelectric sensor-based belt-type high-speed seed guiding device performance monitoring method and system. *Computers and Electronics in Agricultur*e, Vol. 227, pg. 109489.

[21] Zhang, S., Zhu, H., Wang, W., Chen, Y., Zhou, L., Li, M., Wu, J. (2024). Design and optimization test of high-speed seed guide device with conical spiral airflow. *Engenharia Agrícola*, Vol. 44, pg. 20230131